

Compositional modelling of immune response and virus transmission dynamics

William Waites^{1,2}, Matteo Cavaliere³, Vincent Danos^{2,4}, Ruchira Datta⁵,
Rosalind M. Eggo¹, Timothy B. Hallett⁶, David Manheim⁷, Jasmina
Panovska-Griffiths^{8,9}, Timothy W. Russell¹, and Veronika I. Zarnitsyna¹⁰

¹*Centre for Mathematical Modelling of Infectious Disease, London School of Hygiene and Tropical Medicine*

²*School of Informatics, University of Edinburgh*

³*Department of Computing & Mathematics, Manchester Metropolitan University*

⁴*Département d'Informatique, École Normale Supérieure, Paris*

⁵*Datta Enterprises LLC*

⁶*MRC Centre for Global Infectious Disease Analysis, Imperial College London*

⁷*Technion, Israel Institute of Technology*

⁸*The Big Data Institute, Nuffield Department of Medicine, University of Oxford*

⁹*The Queen's College, University of Oxford*

¹⁰*Department of Microbiology and Immunology, Emory University School of Medicine*

November 5, 2021

Abstract

Transmission models for infectious diseases are typically formulated in terms of dynamics between individuals or groups with processes such as disease progression or recovery for each individual captured phenomenologically, without reference to underlying biological processes. Furthermore, the construction of these models is often monolithic: they don't allow one to readily modify the processes involved or include the new ones, or to combine models at different scales. We show how to construct a simple model of immune response to a respiratory virus and a model of transmission using an easily modifiable set of rules allowing further refining and merging the two models together. The immune response model reproduces the expected response curve of PCR testing for COVID-19 and implies a long-tailed distribution of infectiousness reflective of individual heterogeneity. This immune response model, when combined with a transmission model, reproduces the previously reported shift in the population distribution of viral loads along an epidemic trajectory.

1 Introduction

Our starting point in this paper is work by Hellewell and colleagues [28] where they fit a descriptive statistical model to empirical data [29] describing cycle threshold (Ct) values for PCR tests of healthcare workers in England. Rather than describing the data, we aim to get at the mechanism behind it. We begin by asking: what is the simplest, biologically reasonable, process that is sufficient to produce such data? Our answer to this question also produces insights into a possible biological basis for over-dispersion of infections [14] and, when an infection transmission

process is added, the observed shifts in distribution of Ct values during the rising and falling of an epidemic [26].

The method that we use builds upon previous theoretical work in applying techniques first developed for molecular biology [13, 8] to epidemics [53]. These techniques have two important features: *modularity* and *compositionality*. Modularity means that it is possible to create self-contained models, in this case of immune response and transmission that can be individually calibrated and studied. Compositionality means that we can combine these models to create larger ones. This is important for several reasons. Some operations, particularly calibration or fitting to data, are both computationally expensive and critical for real-world applications. We would like, so far as possible, to do these operations once and reuse them.

Beyond the immediate subject-matter of this paper, epidemic trajectories strongly influence and are influenced by processes at several spatial and temporal scales: biology and physiology of the hosts, behaviour and individual choices, policy choices and decision-making, and economic environments to name a few. All of these topics require sophisticated modelling efforts in their own right and a substantial amount of domain expertise. Any strategy for understanding the interplay of these processes that relies on a monolithic approach for modelling is unlikely to be feasible. A modular approach that breaks the large system down into components individually modelled at appropriate scale [57] and then composes them into a model of the whole is much more likely to be effective because the individual components can be small enough to be tractable and enable domain experts to focus their expertise on them. It is equally important that the composition of such models are well-defined if we are to understand the properties of the combined model. We use a method of doing this that builds on a solid foundation of abstract mathematics and category theory [13, 6, 5] to ensure that this is the case, as well as properly representing the biological and epidemiological processes.

Multi-scale models of within- and between-host transmission exist and are recognised as an important line of research [25, 18] and attention has been given to the possibility of composite models for this purpose [19]. Nevertheless, the bulk of infectious disease models [1, 15, 33] are not formulated in ways amenable to composition, perhaps because methods for defining interfaces between models and the interaction of time-scales and concepts of discrete and continuous time remain poorly understood. This remains an important challenge, however progress can be made. There is a longstanding recognition of the need for modular composable models and there are well-developed efforts in this direction in synthetic and systems biology [30, 37, 38, 49, 11, 12, 32, 7].

The remainder of this paper is structured as follows. We first briefly introduce rule-based models in general. We then give our model of adaptive immune response and show the implications for the expected distribution of viral load in terms of time since infection that follows from it. Next, we give the model of transmission and how it is coupled to the immune model and show how the distribution of viral load can be expected to vary according to an epidemic trajectory. Finally we discuss some limitations and future research directions.

2 Rule-based models

The model that we present here, and its constituent sub-models, are formulated as rules. Informally, a rule is the way states of the model change. A rule is a structure with a left-hand side \mathcal{L} , a right-hand side \mathcal{R} , and a rate, k . \mathcal{L} is interpreted as a pattern that matches some part of the system, for example, people with a given characteristic or state or even relationships. \mathcal{R} is an instruction for how the configuration should be changed when that pattern matches; the action

of a rule is to rewrite the configuration of the system so that it evolves over time. In a single simulation step, a single match, or embedding, is chosen from all possible embeddings $\mathcal{E}(\mathcal{L})$ in the graph representing the state of the system, and this embedding is replaced according to the instruction. Thus, a rule encodes many possible transitions (one for each possible embedding) in a continuous time Markov chain (CTMC) where the state-space is all possible graphs. This Markov chain can be simulated with the usual method where the propensity of a rule to operate is given by the number of embeddings, and the rate, $p = k|\mathcal{E}(\mathcal{L})|$. It is possible to sample trajectories from this CTMC exactly without materialising the entire state-space or employing moment-closure techniques [8]. It is also possible to systematically produce ordinary differential equations for the moments of the CTMC, but they are rarely feasible to use in practice for any but the simplest¹ models because of the high dimensionality involved.

The algebra of rules that governs how rules compose is an advanced topic [6], but it is easy to obtain an intuition about how it works with a version of Gillespie’s algorithm [22]. Suppose that we have two rules, r_1 and r_2 . To perform one simulation step for a model with only one rule, we choose one match uniformly at random of the left-hand side of the rule in the system state, replace it with the right-hand side and advance time by an exponentially distributed amount with rate given by the rule’s propensity. Composing the two rules, we perform a step by first choosing which rule to use with probability proportional to their propensities. Having chosen a rule, we then choose a match uniformly at random, do the replacement, and advance time as above with a rate of the total propensity of all rules. This is exactly analogous to simulating a single chemical reaction, except that the “match” and “replace” operations are more complex because they involve searching in and manipulating a graph as opposed to counts of chemical species. Fortunately, we have software that can do this efficiently [8].

In the κ language [13, 8], the configuration of the system is described as a site-graph where vertices are called *agents* (by analogy with the reagents in chemistry, not to be confused with the agents of agent-based models, though some parallels exist), that have *sites* which can have internal *state* and edges are *bonds* between sites of different agents. The biochemical heritage of the formalism is evident from this nomenclature. Figure 1 shows an example agent pattern (e.g. the left-hand side of a rule) pictorially. It consists of two agents, A and B . Both have several binding sites which can be in a unbound (p) or bound (q) state. For patterns, we may not care whether a particular site is bound or not, normally such sites would not be mentioned in a pattern, but when we wish to explicitly depict it, we do this with a half-shaded site (r). A has a site u with internal state x . Where there is no risk of confusion, we may drop the name of the site, as with B which has a nameless binding site and a site with state y . For a thorough explanation of this arrangement in practice in its original setting, the reader may wish to consult Boutillier et al.’s original article [8], as well as our tutorial with examples on the application to infectious diseases [53].

We will use several agent types in the models given below. Agents of type P represent people

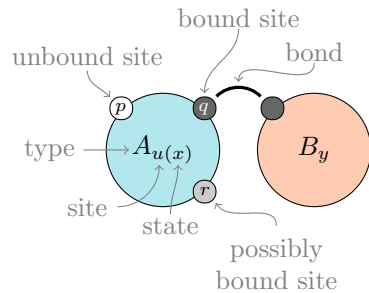


Figure 1: Illustration of an agent pattern with features identified.

¹A typical stratified infectious disease model might have, when rendered as a system of ODEs, at most a hundred dimensions and perhaps a thousand terms. The simple rule-based model that we present here, though finite, corresponds to a system of ODEs with nearly ten thousand dimensions and nearly a hundred million terms.

– chosen rather than I for individual to avoid confusion with individuals in an infectious state as appears in many susceptible, infectious, removed (SIR) style models. Elements of immune response are represented by agents bound to a person, B for B-cells, A for antibody populations. The viral population within a host is represented as an agent of type V . Diagnostic tests of various types are explicitly represented as agents of type T .

3 Adaptive Immune Response

While we use a simplified model here, the general approach can be extended to more complex models of immune response with relatively little effort. We give the model in mathematical form, with explanatory narrative. A methodological observation is that, though we use shape and colour for visual interest, there is an exact correspondence between what is depicted and the machine-readable computer code used for simulation reproduced in Appendix A.

3.1 Viral load

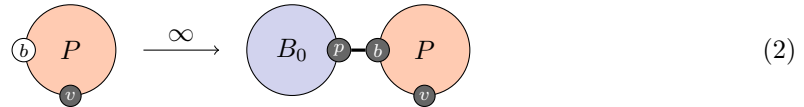
The entire within-host response is driven by replication of the virus. We do not represent individual virions in this model and simply track the size of the virus population. We track this with a counter that represents the logarithm of the population size. Replication is captured simply by incrementing this counter,



up to some maximum. In principle, uncontrolled replication should proceed up to the carrying capacity of the host. For simplicity, we represent this process as simple exponential growth with a maximum limit rather than logistic growth.

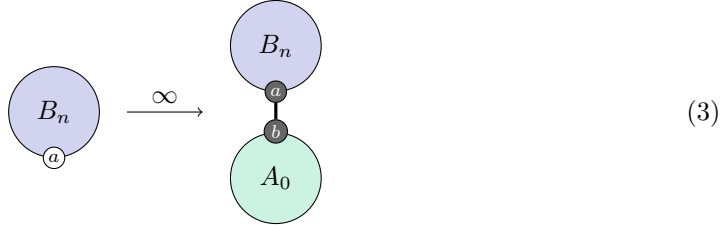
3.2 Initial activation

The peak of viral replication is usually controlled by the innate response together with target cell limitation and further clearance of the virus is controlled by CD8 T-cells and antibodies [2, 45, 41]. In this simplified model, we do not represent the innate response, and we consider notional antibodies as generalised effectors providing the only mechanism for clearance of viral particles. We begin with the activation of B-cells in an infected individual bound to a virus population,



On the left-hand side, the individual has no activated B-cells, and on the right-hand side, they acquire a population of activated B-cells. The subscript on B indicates that all B-cells in this population are naive: they have very low affinity for viral proteins. This process is interpreted as *allocation of a population* of B-cells and not production of the cells themselves. This is somewhat of a computational fiction and is an artefact of the simplifying choice as with the virus population to not track individual cells, but only their count (or in this case, their affinity). The process therefore proceeds immediately, at infinite rate.

The function of B-cells is to produce antibodies. Again, as with the virus population, we do not track individual antibody proteins, we simply track their number, again logarithmically. The second process in the activation of immune response is,



As with the activation of B-cells, this process is interpreted as allocation of a population of antibodies, not the production of antibodies themselves. Antibody production is a separate rule (Equation 5. As with the allocation of a B-cell population, the allocation of an antibody population proceeds immediately.

Once the immune response has been activated, the configuration of the within-host state for an individual is as depicted in Figure 2. The individual is bound to a virus population of a certain size, x (the process by which this happens is exogenous to the immune model), The individual is also bound to a B-cell population with average affinity y , and these B-cells are bound to an associated antibody population with count z .

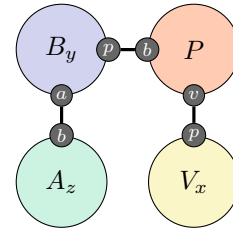
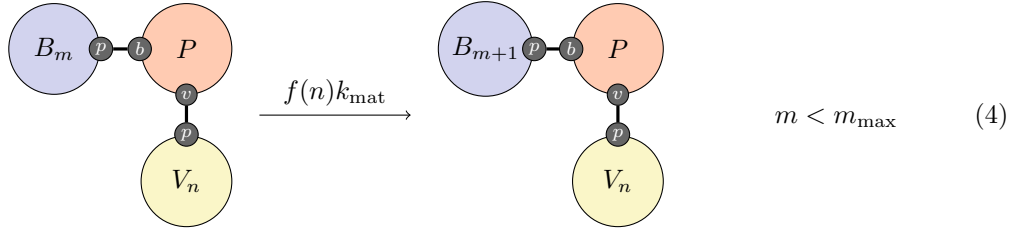


Figure 2: Fully active immune response with viral load x , B-cell affinity y , and antibody count z .

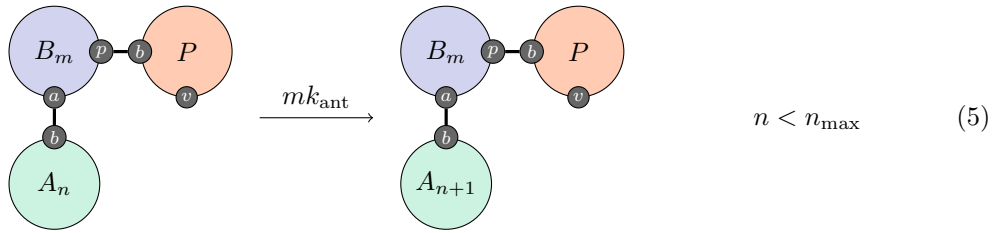
3.3 Immune dynamics

Now we can describe the dynamic processes of the adaptive immune response. They begin with affinity maturation. The process of affinity maturation is only partly understood. Virus-specific B-cells, initially with low affinity, are recruited into special structures called germinal centers (GCs), where their affinity maturation occurs. In GCs, B-cells get stimulated through their B cell receptors by the antigen and undergo the rounds of proliferation with somatic hypermutation (SHM) of their immunoglobulin genes. The cycles of SHM coupled to selection for antigen binding lead to the generation of B-cells of higher affinity. During the affinity maturation process, a fraction of B-cells further differentiate into plasma cells that begin to secrete virus-specific antibodies [36]. Somatic hypermutation continues, and the antibodies produced by the B-cells are iteratively refined and better tuned for binding to the virus. We elide the detail of this fascinating process and treat it phenomenologically at a higher level of abstraction. We reason that in a well-mixed environment, the chance of a B-cell encountering a compatible virion is proportional to some function of the virus population and write,



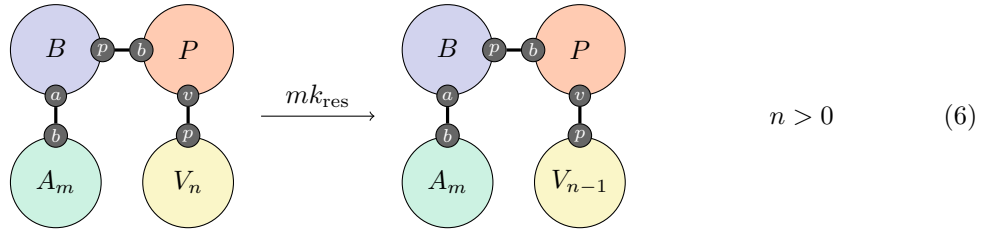
For simplicity, we take $f(n) = n$ and obtain k_{mat} by calibration.

By similar reasoning, antibodies are produced at a rate that we take to be proportional to the affinity,



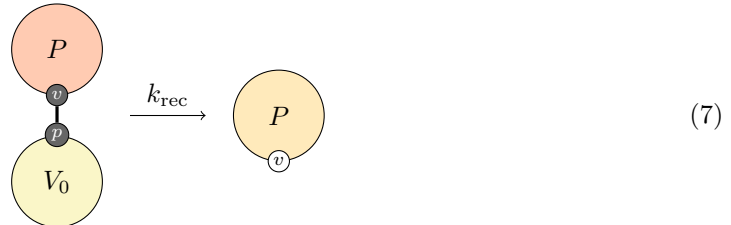
and likewise obtain k_{ant} by calibration. Note that the P agent appears in this rule with an explicitly bound virus population. This is because virus-specific B-cells populations arise and are activated only in the presence of viral proteins; if there are no such proteins, negligible amounts of antibodies (none in our model) are produced.

The action of antibodies is to disable or neutralise virions. We follow a similar pattern and suppose that this happens at a rate proportional to the antibody population,



with the constant of proportionality k_{res} again obtained by calibration.

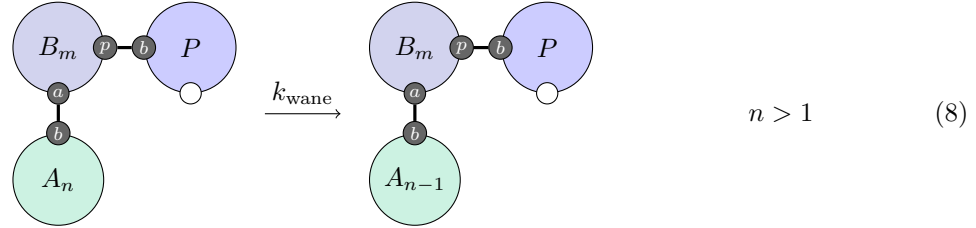
Finally, recovery is said to happen when the virus population drops sufficiently low,



Though we do not need to specify it in this rule, the recovering individual will still have a population of B-cells with some affinity and its associated antibody population. We do not have

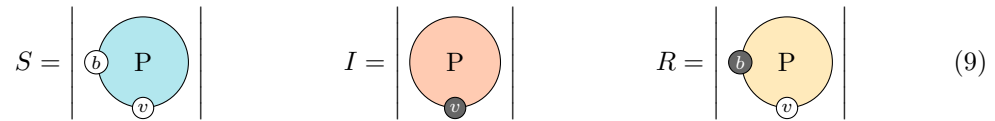
a rule that severs those edges, nor do we have a rule that can decrease affinity. This provides a mechanism for immune memory. If a previously infected individual is exposed to the virus again, they may have a population of antibodies that can immediately dispatch it and if they do not, their B-cells can produce them.

Finally, we include a simple rule very similar to the above for waning, where the antibody population decreases slowly when the individual does not have a virus population,



3.4 Connection to compartments

In epidemiological models it is traditional to subdivide the population into susceptible individuals, removed individuals, and one or more compartments of individuals in different states of incubation or infectiousness. Even with individual- or agent-based models, this classification of individuals is commonly used. There is a natural way to make the connection to these concepts simply by counting configurations of individuals and their immune response. This is done by defining *observables* that count the number of embeddings of a pattern similar to the operation of the left-hand side of a rule,



where the vertical bars are used in the sense of cardinality of a set – the set of embeddings induced by the patterns. A susceptible individual is one who has no virus population and no established immune memory. An infected or infectious individual has a virus population regardless of the state of their immune response and a recovered or removed individual has no virus population but does have established immune memory. These correspondences of course only give a coarse picture of the expected dynamics: they do not consider the robustness of the immune memory or the degree of infectiousness. This coarseness is the reason that, if we were to work at the level of compartments (i.e. high-level disease progression states whether in a compartmental model or otherwise), we would be required to formulate processes in terms of complicated distributions chosen either by hypothesis or empirically. Here, we do not need to do that because we have access to a fine-grained account of adaptive immune response. It is nevertheless useful to have a view of the dynamics of this model that is comparable to the more common representation.

3.5 Empirical validation

It is easy to see that viral load – the quantity of virus carried by a host – must vary over the course of the disease. At the time immediately prior to infection, there is no virus present. At some future time after the infection has been cleared, there is likewise no virus present. At some

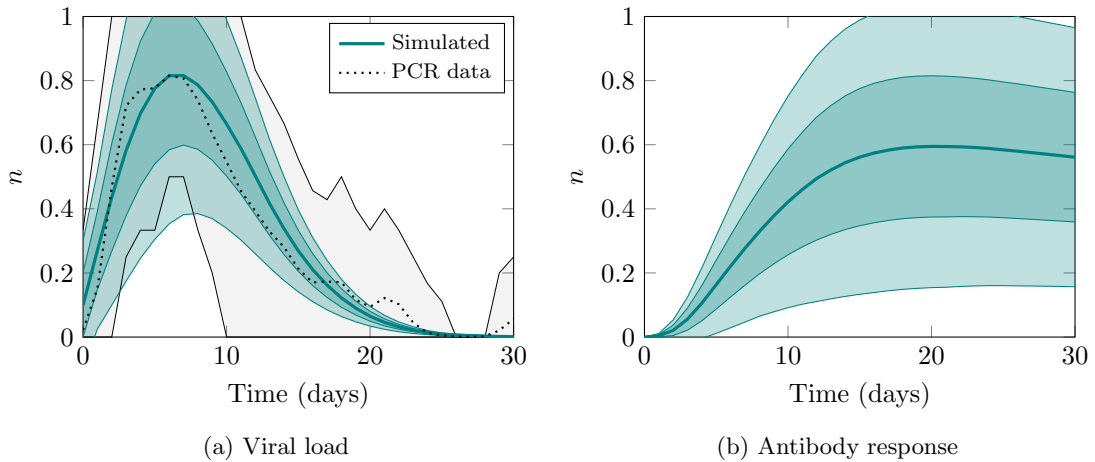


Figure 3: Within-host immune dynamics sampled from a population of 10,000. The system is fit to PCR response data response as reported by Hellewell et al. [28]. Underlying processes of virus replication, affinity maturation, antibody production and virus neutralisation reproduce the characteristically asymmetric viral load curve (3a) and an antibody response curve (3b) that lags viral load. The vertical axis in both figures is measured in arbitrary logarithmic units.

time in between there must be some non-zero amount of virus present because that is the meaning of infection. Therefore, viral load must have been increasing for some of that time, and decreasing for some of that time and it must have had a maximum for some time between these phases. Whilst there is no *a priori* guarantee that there must be only one occurrence of each of these phases, the simplest behaviour would be a single increasing phase, a peak, and a decreasing phase. This is precisely what we observe empirically through assays that are sensitive to the presence of virus itself (e.g. PCR) or viral proteins (e.g. antigen) [51, 56, 10, 28]. Furthermore, because the various immune processes that eventually suppress the population of virions take time to develop, any increase in antibody products must lag behind an initial increase in viral load, again, precisely what is observed with antibody assays [51, 56, 10].

The adaptive immune response model reproduces the above observations from the underlying processes. We calibrated the model with the Approximate Bayesian Computation (ABC) method using a Root Mean Square (RMS) distance relative to the mean PCR test response for SARS-CoV-2 infection as reported by Hellewell et al. [28] based on data from a study of health workers in England [29]. The fitting procedure is computationally expensive, however it need only be performed once: the calibrated immune model stands on its own and for many uses it can be combined with other models without the necessity to repeat this expensive procedure. The resulting viral load and antibody response curves for a population of 10,000 individuals are shown in Figure 3 and the reference data together with its 95% credible interval is also shown in Figure 3a.

The measurement scale used in Figure 3 is logarithmic and truncated. In the adaptive immune response model the populations of virions and antibodies are both represented as an integer, n . This integer n is interpreted as the logarithm of the size of the population. The justification for this interpretation is the nature of testing with PCR and laboratory assays. Quantitative results are obtained by either successive dilutions (titrations) or by successively culturing under

conditions that permit exponential growth. The cycle threshold value reported for PCR tests, for example, is the number of growth cycles required to detect RNA from the virus, and can be interpreted (with a change of sign, up to a constant factor) as the logarithm of the initial amount of RNA. Similar reasoning applies to the titres reported from laboratory assays for antibodies or antigens. In both cases, a positive or negative result is simply a statement that a threshold value has been passed. The measurement scale n that we use is truncated for practical reasons at a maximum value n_{\max} . The rates at which various processes in the model occur are expressed in terms proportional to n for the various entities involved. This interpretation, together with the fitting procedure as described rests on the following assumption connecting the mechanistic model to the empirical test data: *the rate of positive test results is proportional to the logarithm of the viral population.*

3.6 Viral load distribution

Figure 4 shows data from the same simulation of 10,000 individuals. All individuals are infected at the beginning of the simulation. It depicts the probability distributions of an individual to have a particular viral load as measured on the scale that we have defined, from 0 to $n_{\max} = 20$. We observe a wave of probability starting with a certainty that all individuals have a viral load $n = 1$, with viral load increasing as time progresses. After about 10 days, a significant result appears: a long-tailed distribution where an ever-smaller proportion of the population has a large viral load. This is significant because it suggests a biological basis for the phenomenon of over-dispersion in infectiousness, typically captured in infectious disease models by asserting an appropriately parametrised Gamma distribution of infectiousness [14]. By the end of this 14 day sequence, 80% of viral load is concentrated in approximately 20% of the population and by day 21 this has shrunk to 3%. On average, over the entire 30 day period of the simulation, 80% of the viral load is concentrated in 21% of the population. Teasing out the implications of these results can shed some light on the phenomenon of superspreading individuals. On the one hand, increasing viral load may increase the chance of an individual transmitting virus in any given encounter. On the other hand, increasing viral load may also increase the chance of developing symptoms, to the extent that the individual would be more likely to self-isolate. Thus the chance of encounters occurring would diminish. The product of these two factors gives the overall chance of transmission. The interplay between these two factors: transmissibility upon a given encounter (increasing with viral load) and chance of encounter (decreasing with viral load) may result in the overall chance of transmission being a concave function of viral load, with a peak at an intermediate viral load. Factors that increase the chance of encounter at any given viral load (such as lack of paid sick leave from a public-facing job) would shift the peak of the function right (to a higher viral load). However, if an individual with a large viral load is present in a situation where transmission is likely, then it is reasonable to expect that a superspreading event may occur [24].

In passing, we observe that the processes in the adaptive immune response model are more than are strictly required to reproduce this kind of long tailed distribution of viral load. It is possible to show that a simpler model where load simply increases incrementally and then decreases, with the turning point chosen stochastically will produce a similar result. Such a simple model, however, lacks biological realism and fails to provide a causal or mechanistic account of the phenomenon.

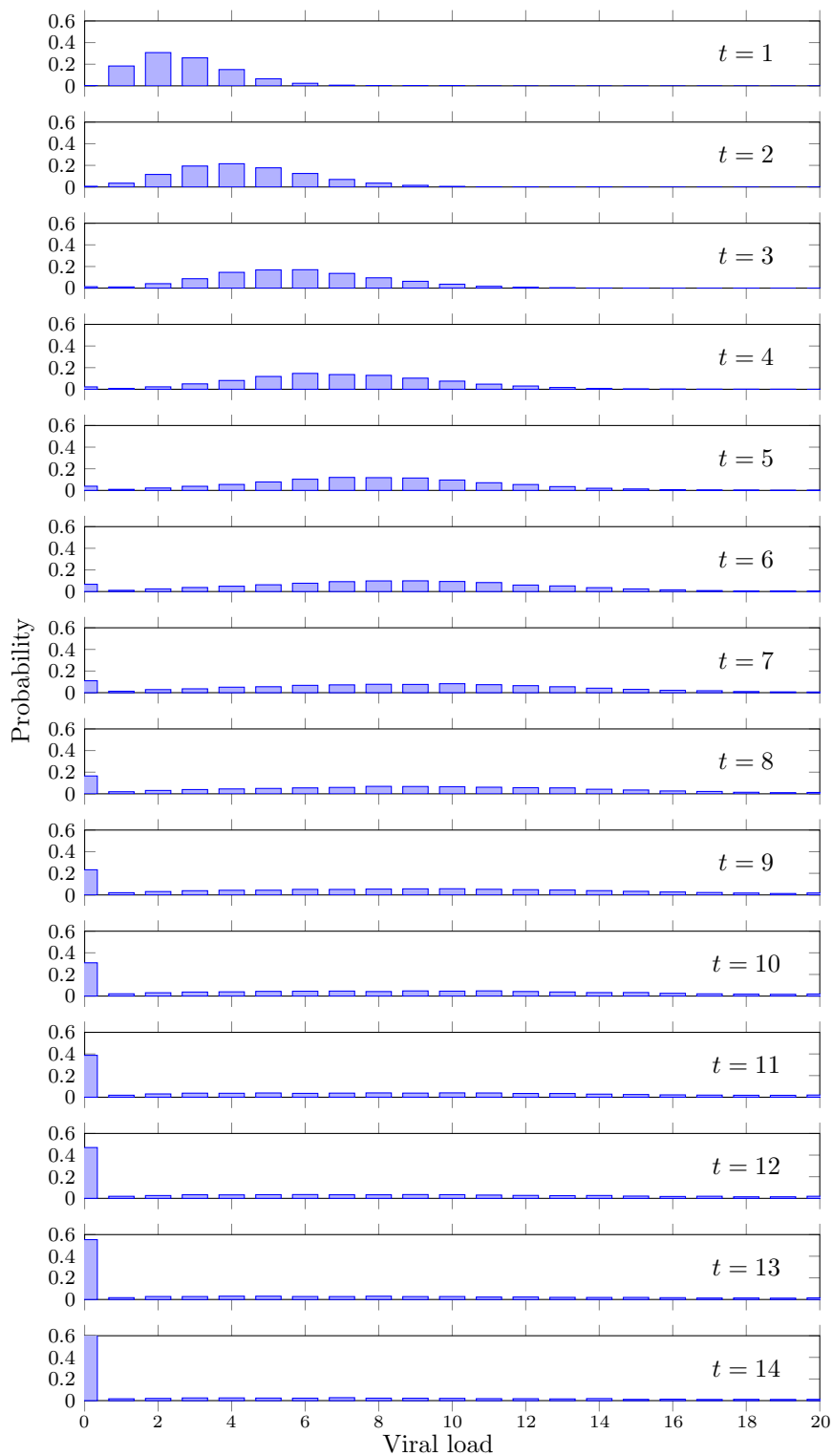
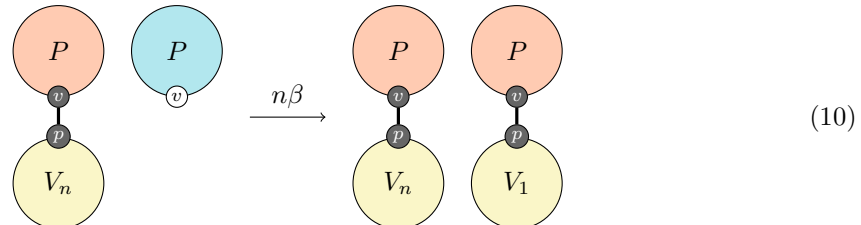


Figure 4: Timeseries of probability distributions of having a viral load on a scale of 0 to $n_{\max} = 20$, from the same simulation of 10,000 individuals as Figure 3. By day 14, 80% of viral load is concentrated in approximately 20% of individuals.

4 Transmission dynamics

Unlike immune response which occurs within individuals, transmission is a population-level process that occurs between individuals. With the above formulation in hand, a simple model of transmission is very natural,

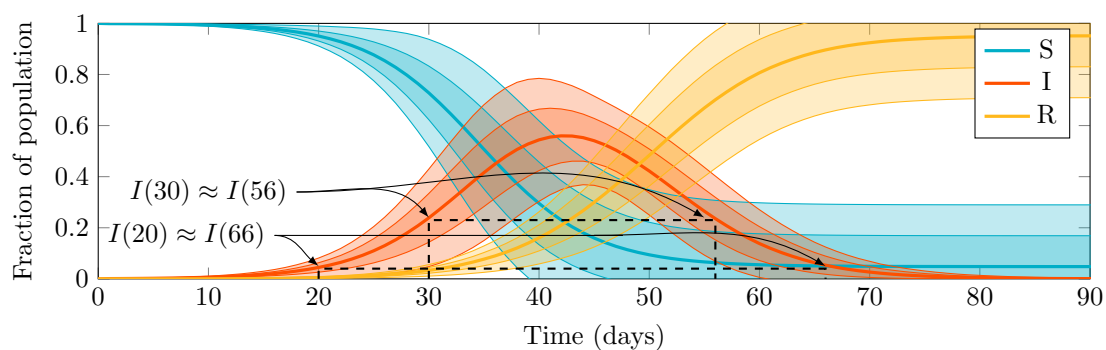


This says that an individual with some virus encounters an individual without the virus (this implies well-mixed, mass action kinetics) and as a result of that interaction, the second individual gets a small virus population.

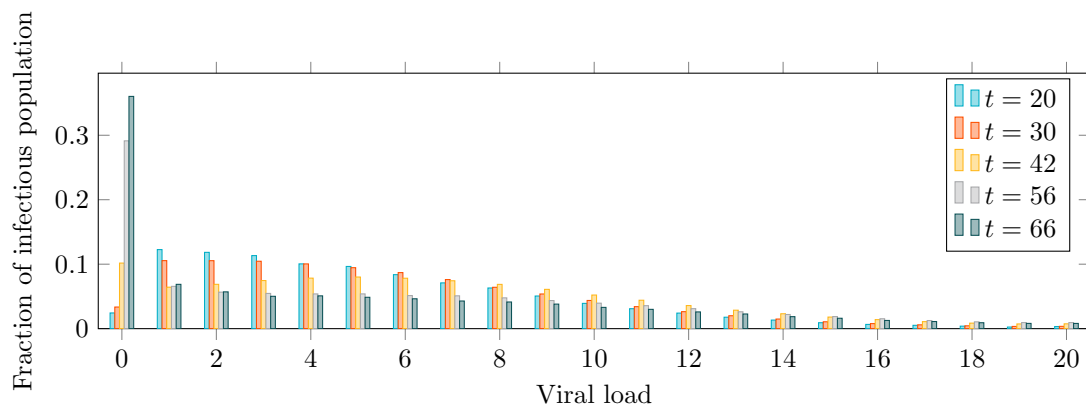
Note in particular that it is not necessary to speak of any previous infections experienced by the second individual. Nothing corresponding to immunity is required here because *if* an individual with established immune memory is exposed to the virus, *then* their immune response will simply be very rapid and they will clear the virus quickly. There is no need to impose an *a priori* restriction on individuals being exposed more than once or to assert a sharp distinction between individuals that are “immune” and those that are not.

Figure 5a shows the epidemic curve produced by the combined transmission and immune model according to the observables (cf Section 33.4) corresponding to the standard epidemic model compartments. The rate parameter β in Equation 10 is fit so as to produce an epidemic with a basic reproduction number $R_0 = 3$, typical of the ancestral strain of SARS-CoV-2 in a Western European setting. Determining a precise value for R_0 and hence β is setting-specific, strongly affected by behaviour, and of only peripheral interest here. Two pairs of time points are marked on the figure, corresponding to the times at which, on average, the same number of individuals are infected as the epidemic rises and falls. The first pair, $t \in \{20, 66\}$, is when a small number of individuals are infected and the second, $t \in \{30, 56\}$ when a much larger number are. Finally, we notice that the epidemic is stationary (i.e. peaks, is neither rising nor falling) around $t = 42$.

Let us look at the viral load distributions at these chosen time points in more detail, Figure 5b. We see that the distributions differ substantially. For a rising epidemic ($t \in \{20, 30\}$), the bulk of the probability mass is shifted towards the left, indicating a lower viral load. As individuals become infected faster and faster, there are more individuals who are at an early stage in the course of their infection. Recall from Figure 3a that we expect a peak viral load perhaps a week after initial infection and then a slow decay over the subsequent several weeks. On the other hand, for a falling epidemic ($t \in \{56, 66\}$), the probability distribution is bimodal. Much of the probability mass is concentrated in the lowest viral load as many individuals are on the point of recovery. However, a significant amount of probability mass is present in high viral loads reflecting individuals with developed infections and slowly decaying viral loads. A similar effect was noted by Hay and colleagues [26] who showed that rising and falling epidemics can be distinguished by looking at the distribution of cycle threshold values in PCR tests and that this can, in fact, be used to estimate the time-varying reproduction number $R(t)$ in a population. We recover this result as a consequence of the immune dynamics in the model.



(a) Epidemic curve showing the susceptible (S), infectious (I) and removed (R) observables for a population of 10000 individuals calibrated for a reproduction number of 3. Envelopes show one and two standard deviations over 128 simulations. Marked on the graph are two pairs of time points where the mean number of infectious individuals are equal as the epidemic rises and falls.



(b) Viral load distribution at different points of the epidemic trajectory showing a rising $t \in \{20, 30\}$, stationary $t = 42$, and falling $t \in \{56, 66\}$ epidemic. Viral load in arbitrary logarithmic units. The probability masses of distributions are shifted to the left (lower viral loads) for a rising epidemic and the distribution for a falling epidemic is in fact bimodal with most infected individuals on the point of recovery but a significant number with slowly decaying high viral loads.

Figure 5: Epidemic curve and viral load distributions for a rising, stationary and falling epidemic.

5 Discussion

Previous work on models, both across domains and for infectious disease modelling specifically [40], have suggested that there are various features which make models more useful for different tasks. For infectious disease modelling, useful features include predictive accuracy, ability to effectively model historic behaviour and predict the outcomes of future interventions in a way that reveals causality, flexibility to update both the model structure and calibration of parameters as new information becomes available, computational tractability, and ease of explanation to policymakers and the public. The approach presented here has significant advantages across many of these desiderata though there is also still work to be done. Our emphasis on *modularity* and *compositionality* facilitates the flexibility to update model structure: individual rules or entire submodels can be changed or substituted locally, without requiring global changes. Indeed it is possible to analyse the dependencies between rules to determine precisely the extent to which modifications to one part of the model may require modification to other parts. The modular structure means that it is often possible to calibrate submodels individually, saving the great computational expense of performing this operation for all parameters, which is often necessary for monolithic models.

Additionally, this modular and compositional approach facilitates multidisciplinary collaboration. Infectious disease modelling, immunological modelling, modelling of behaviour and economies and supply chains all require a substantial amount of domain expertise and each has a substantial literature of sophisticated models particular to that field. By encapsulating the models and paying attention to the (often unclear or fuzzy) boundaries between them, there is hope for constructing larger, richer models without the tight coupling required by monolithic approaches. Not only that, but we can mix and match. Perhaps a particular immune model is computationally intensive and the cost outweighs the benefit for the question at hand; it can simply be replaced with a simpler one with a compatible interface. Quantitative models of behaviour are difficult to calibrate because data to relate them to ground truth are scarce. This becomes a surmountable obstacle because one can simply use several; such models are simply assumptions of dynamics about which our knowledge is limited so we can evaluate the entire system under different sets of assumptions ranging from simple to very sophisticated. The ability to slot these different models into the same context, can allow us to take advantage of decision-making frameworks that incorporate multiple predictors, each of which individually may be “weak” (i.e., low-confidence). *Boosting* is an example of such an ensemble method [46] [17]. The structure described is that of *Open Systems*, a concept that dates at least to von Bertalanffy’s work in 1950 [52]. Recent advances in mathematics for interacting systems [16] stochastic rewriting systems [5] (of which the models presented in this paper are examples) and specific kinds of open systems such as Petri nets [4, 3], and economic games [21, 27] are placing these ideas on solid theoretical ground for computation. By leveraging these theoretical advances we stand to make great practical benefit in multi-scale and multi-disciplinary modelling. Even more ambitiously, such approaches allow representations used in sets of models to scale from physics to chemistry to biology to epidemiology, pharmacology, and more. This is consistent with similar approaches being taken in systems biology [42], pharmacology [31], and (bio)chemical engineering [39]. Of course, any one model or set of models will occupy only a small part of this spectrum; however, through composition and selection of models, many types of interdisciplinary and trans-disciplinary modelling approaches become possible, enabling us to address an immense variety of questions.

There are numerous challenges to fully realising this dream. A major obstacle is that there is, at present, no developed theory of how the behaviour of one model influences the parameters of

others - though some work in other fields is beginning to address this [43]. This challenge is reflected in our discourse above where we explicitly choose how rates (of transmission, say) depend on values (e.g. viral load) that are produced as a result of a different model. This pattern, where the state of the system as described by one process influences the parameters of a different process, is very common and, at present, must simply be handled manually. A promising approach is that of Open Games [20, 21, 27] where the composition of games is defined for *all possible* utility functions – essentially parametrisation of the games. We could imagine Petri nets with rates or more general kinds of stochastic rewriting systems taking a similar approach where their composition defined for all possible rate functions with specialisation to particular choices of rate function done post-hoc once the complete model is assembled. The combination of Open Games and Open Stochastic Rewriting Systems is potentially very powerful. Game theory is a unifying framework that can be used to underpin statistics [55], machine learning [47] [9], microeconomic theory [34] and the behavioural sciences [23], and is already used in a more specialised way in epidemiological modelling [44]. The Open Games formalism for compositional modelling supports combining submodels that may include games at different levels; for instance, within-host models where the agents are immune cells and virions within an organism, with between-host models where the agents are various organisms within a social milieu. This speculation suggests a path for incorporating epidemic models (which may themselves include game theory) into more overarching game-theoretic accounts in a principled way.

Another challenge is that the formulation of these models in the standard κ calculus permits only well-mixed interactions and site-graphs. In other work [54], we have extended the language to support more general graphs of the kind that are needed for epidemic models on networks, but a further extension to capture explicit hierarchical notions of space as suggested in work on stochastic bigraphs [35] would be beneficial.

The model of adaptive immune response given here is greatly simplified and we have provided no more than a vestigial model of the innate response. For COVID-19, it appears that the innate response plays an important role in whether an individual will recover after the initial acute phase of the disease or go on to develop severe disease [48]. The precise reason for this is not known. Equally, it is an open question why some individuals appear to recover completely and others develop persistent and varied symptoms known as “long covid” [50]. These persistent symptoms may be rooted in immune response or could have a physiological explanation. In both cases, there is hope that more sophisticated models of immune response and physiology could provide the necessary insight. Beyond these immediate questions, multi-scale, multi-system models are relevant not only for understanding population-level dynamics but for drug discovery and precision treatment of individuals. Modular and compositional modelling techniques such as we demonstrate here provide a method for taming the substantial complexity involved.

Ethics The ethical approval for the human data used in this analysis is detailed in the original manuscript reporting the study outcomes [29]. It states that: ‘The study protocol was approved by the NHS Health Research Authority (ref 20/SC/0147) on 26 March 2020. Ethical oversight was provided by the South Central Berkshire Research Ethics Committee’.

Data Access Source code is available at:

<https://git.sr.ht/~wwaites/immune-transmission>

Calibration data and sampled trajectories are available at:

<https://datashare.ed.ac.uk/handle/10283/4056>

Author Contributions WW wrote the software, conducted the simulations, and wrote the initial draft of this article. WW, MC, VD and TH designed the numerical experiments. TR contributed empirical data. All authors wrote and revised the manuscript.

Competing Interests The authors declare no competing interests

Funding WW, DM and TH acknowledge support from the Foundation for Innovative New Diagnostics. WW and RME were supported by MRC grant MR/V027956/1. DM also acknowledges support from the Center for Effective Altruism’s Long-Term Future Fund.

Acknowledgements The authors would like to thank members of the CMMID COVID-19 Working Group for constructive feedback on drafts of this article. Simulations performed using resources provided by the Cambridge Service for Data Driven Discovery (CSD3) operated by the University of Cambridge Research Computing Service.

Disclaimer The funders had no role in the design, conduct or analysis of the study or the decision to publish.

References

- [1] Sam Abbott, Joel Hellewell, Katharine Sherratt, Katelyn Gostic, Joe Hickson, Hamada S. Badr, Michael DeWitt, Robin Thompson, EpiForecasts, and Sebastian Funk. EpiNow2: Estimate Real-Time Case Counts and Time-Varying Epidemiological Parameters, 2020.
- [2] Prasith Baccam, Catherine Beauchemin, Catherine A. Macken, Frederick G. Hayden, and Alan S. Perelson. Kinetics of Influenza A Virus Infection in Humans. *Journal of Virology*, 80(15):7590–7599, August 2006. ISSN 0022-538X, 1098-5514. doi:[10.1128/JVI.01623-05](https://doi.org/10.1128/JVI.01623-05).
- [3] John C. Baez and Kenny Courser. Structured cospans. *Theory and Applications of Categories*, 35(48):1771–1822, October 2020. URL <http://www.tac.mta.ca/tac/volumes/35/48/35-48abs.html>.
- [4] John C. Baez and Jade Master. Open Petri nets. *Mathematical Structures in Computer Science*, 30(3):314–341, March 2020. ISSN 0960-1295, 1469-8072. doi:[10.1017/S0960129520000043](https://doi.org/10.1017/S0960129520000043).
- [5] Nicolas Behr and Pawel Sobocinski. Rule Algebras for Adhesive Categories. *Logical Methods in Computer Science ; Volume 16*, page Issue 3 ; 18605974, July 2020. ISSN 1860-5974. doi:[10.23638/LMCS-16\(3:2\)2020](https://doi.org/10.23638/LMCS-16(3:2)2020).
- [6] Nicolas Behr, Vincent Danos, and Ilias Garnier. Stochastic mechanics of graph rewriting. In *Proceedings of the 31st Annual ACM/IEEE Symposium on Logic in Computer Science, LICS '16*, pages 46–55, New York, NY, USA, July 2016. Association for Computing Machinery. ISBN 978-1-4503-4391-6. doi:[10.1145/2933575.2934537](https://doi.org/10.1145/2933575.2934537).
- [7] Michael L. Blinov, John H. Gennari, Jonathan R. Karr, Ion I. Moraru, David P. Nickerson, and Herbert M. Sauro. Practical resources for enhancing the reproducibility of mechanistic modeling in systems biology. *Current Opinion in Systems Biology*, 27:100350, September 2021. ISSN 2452-3100. doi:[10.1016/j.coisb.2021.06.001](https://doi.org/10.1016/j.coisb.2021.06.001).

- [8] Pierre Boutillier, Mutaamba Maasha, Xing Li, Héctor F. Medina-Abarca, Jean Krivine, Jérôme Feret, Ioana Cristescu, Angus G. Forbes, and Walter Fontana. The Kappa platform for rule-based modeling. *Bioinformatics*, 34(13):i583–i592, July 2018. ISSN 1367-4803. doi:[10.1093/bioinformatics/bty272](https://doi.org/10.1093/bioinformatics/bty272).
- [9] N. Cesa-Bianchi and G. Lugosi. *Prediction, Learning, and Games*. Cambridge University Press, 2006. ISBN 9780521841085. URL <https://books.google.com/books?id=Je9tngEACAAJ>.
- [10] Muge Cevik, Krutika Kuppalli, Jason Kindrachuk, and Malik Peiris. Virology, transmission, and pathogenesis of SARS-CoV-2. *BMJ*, 371:m3862, October 2020. ISSN 1756-1833. doi:[10.1136/bmj.m3862](https://doi.org/10.1136/bmj.m3862).
- [11] Vijayalakshmi Chelliah, Camille Laibe, and Nicolas Le Novère. BioModels Database: A Repository of Mathematical Models of Biological Processes. In Maria Victoria Schneider, editor, *In Silico Systems Biology, Methods in Molecular Biology*. Humana Press, Totowa, NJ, 2013. ISBN 978-1-62703-450-0. doi:[10.1007/978-1-62703-450-0_10](https://doi.org/10.1007/978-1-62703-450-0_10).
- [12] Michael Clerx, Michael T. Cooling, Jonathan Cooper, Alan Garny, Keri Moyle, David P. Nickerson, Poul M. F. Nielsen, and Hugh Sorby. CellML 2.0. *Journal of Integrative Bioinformatics*, 17(2-3), June 2020. ISSN 1613-4516. doi:[10.1515/jib-2020-0021](https://doi.org/10.1515/jib-2020-0021). URL <https://www.degruyter.com/document/doi/10.1515/jib-2020-0021/html>.
- [13] Vincent Danos and Cosimo Laneve. Formal molecular biology. *Theoretical Computer Science*, 325(1):69–110, September 2004. ISSN 0304-3975. doi:[10.1016/j.tcs.2004.03.065](https://doi.org/10.1016/j.tcs.2004.03.065).
- [14] Akira Endo, Centre for the Mathematical Modelling of Infectious Diseases COVID-19 Working Group, Sam Abbott, Adam J. Kucharski, and Sebastian Funk. Estimating the overdispersion in COVID-19 transmission using outbreak sizes outside China. *Wellcome Open Research*, 5:67, July 2020. ISSN 2398-502X. doi:[10.12688/wellcomeopenres.15842.3](https://doi.org/10.12688/wellcomeopenres.15842.3).
- [15] N. Ferguson, G. Nedjati Gilani, and D. Laydon. COVID-19 CovidSim microsimulation model, April 2020. URL <http://spiral.imperial.ac.uk/handle/10044/1/79647>.
- [16] José Luiz Fiadeiro and Vincent Schmitt. Structured Co-spans: An Algebra of Interaction Protocols. In Till Mossakowski, Ugo Montanari, and Magne Haveraaen, editors, *Algebra and Coalgebra in Computer Science*, Lecture Notes in Computer Science, Berlin, Heidelberg, 2007. Springer. ISBN 978-3-540-73859-6. doi:[10.1007/978-3-540-73859-6_14](https://doi.org/10.1007/978-3-540-73859-6_14).
- [17] Y. Freund. Boosting a weak learning algorithm by majority. *Information and Computation*, 121(2):256–285, 1995. ISSN 0890-5401. doi:<https://doi.org/10.1006/inco.1995.1136>. URL <https://www.sciencedirect.com/science/article/pii/S0890540185711364>.
- [18] Rebecca B. Garabed, Anna Jolles, Winston Garira, Cristina Lanzas, Juan Gutierrez, and Grzegorz Rempala. Multi-scale dynamics of infectious diseases. *Interface Focus*, 10(1):20190118, February 2020. ISSN 2042-8898, 2042-8901. doi:[10.1098/rsfs.2019.0118](https://doi.org/10.1098/rsfs.2019.0118).
- [19] Winston Garira. A complete categorization of multiscale models of infectious disease systems. *Journal of Biological Dynamics*, 11(1):378–435, January 2017. ISSN 1751-3758, 1751-3766. doi:[10.1080/17513758.2017.1367849](https://doi.org/10.1080/17513758.2017.1367849).
- [20] Neil Ghani, Jules Hedges, Viktor Winschel, and Philipp Zahn. Compositional game theory. In *Proceedings of the 33rd Annual ACM/IEEE Symposium on Logic in Computer Science, LICS '18*, page 472–481, New York, NY, USA, 2018. Association for Computing Machinery. ISBN 9781450355834. doi:[10.1145/3209108.3209165](https://doi.org/10.1145/3209108.3209165). URL <https://doi.org/10.1145/3209108.3209165>.

- [21] Neil Ghani, Clemens Kupke, Alasdair Lambert, and Fredrik Nordvall Forsberg. A compositional treatment of iterated open games. *Theoretical Computer Science*, 741:48–57, September 2018. ISSN 03043975. doi:[10.1016/j.tcs.2018.05.026](https://doi.org/10.1016/j.tcs.2018.05.026).
- [22] Daniel T. Gillespie. Exact stochastic simulation of coupled chemical reactions. *The Journal of Physical Chemistry*, 81(25):2340–2361, December 1977. ISSN 0022-3654. doi:[10.1021/j100540a008](https://doi.org/10.1021/j100540a008).
- [23] H. Gintis. *The Bounds of Reason: Game Theory and the Unification of the Behavioral Sciences - Revised Edition*. Princeton University Press, 2014. ISBN 9781400851348. URL <https://books.google.com/books?id=fFb0AgAAQBAJ>.
- [24] Ashish Goyal, Daniel B Reeves, E Fabian Cardozo-Ojeda, Joshua T Schiffer, and Bryan T Mayer. Viral load and contact heterogeneity predict SARS-CoV-2 transmission and super-spreading events. *eLife*, 10:e63537, February 2021. ISSN 2050-084X. doi:[10.7554/eLife.63537](https://doi.org/10.7554/eLife.63537).
- [25] Andreas Handel and Pejman Rohani. Crossing the scale from within-host infection dynamics to between-host transmission fitness: a discussion of current assumptions and knowledge. *Philosophical Transactions of the Royal Society B: Biological Sciences*, 370(1675):20140302, August 2015. ISSN 0962-8436, 1471-2970. doi:[10.1098/rstb.2014.0302](https://doi.org/10.1098/rstb.2014.0302).
- [26] James A. Hay, Lee Kennedy-Shaffer, Sanjat Kanjilal, Niall J. Lennon, Stacey B. Gabriel, Marc Lipsitch, and Michael J. Mina. Estimating epidemiologic dynamics from cross-sectional viral load distributions. *Science*, June 2021. ISSN 0036-8075, 1095-9203. doi:[10.1126/science.abh0635](https://doi.org/10.1126/science.abh0635). Publisher: American Association for the Advancement of Science Section: Research Article.
- [27] Jules Hedges. Morphisms of Open Games. *Electronic Notes in Theoretical Computer Science*, 341:151–177, December 2018. ISSN 1571-0661. doi:[10.1016/j.entcs.2018.11.008](https://doi.org/10.1016/j.entcs.2018.11.008).
- [28] Joel Hellewell, Timothy W. Russell, Rebecca Matthews, Abigail Severn, Sajida Adam, Louise Enfield, Angela McBride, Kathleen Gärtner, Sarah Edwards, Fabiana Lorencatto, Susan Michie, Ed Manley, Maryam Shahmanesh, Hinal Lukha, Paulina Prymas, Hazel McBain, Robert Shortman, Leigh Wood, Claudia Davies, Bethany Williams, Emilie Sanchez, Daniel Frampton, Matthew Byott, Stavroula M. Paraskevopoulou, Elise Crayton, Carly Meyer, Nina Vora, Triantafylia Gkouleli, Andrea Stoltenberg, Veronica Ranieri, Tom Byrne, Dan Lewer, Andrew Hayward, Richard Gilson, Naomi Walker, Aaron Ferron, Aaron Sait, Abhinay Ramaprasad, Abigail Perrin, Adam Sateriale, Adrienne E. Sullivan, Aileen Nelson, Akshay Madoo, Alana Burrell, Aleksandra Pajak, Alessandra Gaiba, Alice Rossi, Alida Avola, Alison Dibbs, Alison Taylor-Beadling, Alize Proust, Almaz Huseynova, Amar Pabari, Amelia Edwards, Amy Strange, Ana Cardoso, Ana Agua-Doce, Ana Perez Caballero, Anabel Guedan, Anastacio King Spert Teixeira, Anastasia Moraiti, Andreas Wack, Andrew Riddell, Andrew Buckton, Andrew Levett, Andrew Rowan, Angela Rodgers, Ania Kucharska, Anja Schlott, Annachiara Rosa, Annalisa D’Avola, Anne O’Garra, Anthony Gait, Antony Fearn, Beatriz Montaner, Belen Gomez Dominguez, Berta Terré Torras, Beth Hoskins, Bishara Marzook, Bobbi Clayton, Bruno Frederico, Caetano Reis e Sousa, Caitlin Barns-Jenkins, Carlos M. Minutti, Caroline Oedekoven, Catharina Wenman, Catherine Lambe, Catherine Moore, Catherine F. Houlihan, Charles Swanton, Chelsea Sawyer, Chloe Rouston, Chris Ekin, Christophe Queval, Christopher Earl, Claire Brooks, Claire Walder, Clare Beesley, Claudio Bussi, Clementina Cobolli Gigli, Clinda Puvirajasinghe, Cristina Naceur-Lombardelli, Dan Fitz, Daniel M. Snell, Dara Davison, David Moore, Davide Zecchin, Deborah Hughes, Deborah Jackson, Dhruva Biswas, Dimitrios Evangelopoulos, Dominique Bonnet, Edel C. McNamara, Edina Schweighoffer, Effie Taylor, Efthymios Fidanis, Eleni Nastouli, Elizabeth Horton, Ellen Knuepfer, Emine Hatipoglu, Emma Russell, Emma Ashton, Enzo ZPoirier, Erik Sahai, Fatima Sardar, Faye Bowker, Fernanda Teixeira Subtil, Fiona McKay, Fiona Byrne, Fiona Hackett, Fiona Roberts, Francesca Torelli, Ganka Bineva-Todd, Gavin Kelly, Gee Yen Shin, Genevieve Barr, George Kassiotis, Georgina H. Cornish, Gita Mistry, Graeme

Hewitt, Graham Clark, Gunes Taylor, Hadija Trojer, Harriet B. Taylor, Hector Huerga Encabo, Heledd Davies, Helen M. Golding, Hon-Wing Liu, Hui Gong, Jacki Goldman, Jacqueline Hoyle, James Fleming, James I. MacRae, James M. Polke, James M. A. Turner, Jane Hughes, Jean D. O’Leary, Jernej Ule, Jerome Nicod, Jessica Olsen, Jessica Diring, Jill A. Saunders, Jim Aitken, Jimena Perez-Lloret, Joachim M. Matz, Joanna Campbell, Joe Shaw, John Matthews, Johnathan Canton, Joshua Hope, Joshua Wright, Joyita Mukherjee, Judith Heaney, Julian AZagalak, Julie A. Marczak, Karen Ambrose, Karen Vousden, Katarzyna Sala, Kayleigh Richardson, Kerol Bartolovic, Kevin W. Ng, Konstantinos Kousis, Kylie Montgomery, Laura Churchward, Laura Cubitt, Laura Peces-Barba Castano, Laura Reed, Laura E. McCoy, Lauren Wynne, Leigh Jones, Liam Gaul, Lisa Levett, Lotte Carr, Louisa Steel, Louise Busby, Louise Howitt, Louise Kiely, Lucia Moreira-Teixeira, Lucia Prieto-Godino, Lucy Jenkins, Luiz Carvalho, Luke Nightingale, Luke Williams, Lyn Healy, Magali S. Perrault, Malgorzata Broncel, Marc Pollitt, Marcel Levi, Margaret Crawford, Margaux Silvestre, Maria Greco, Mariam Jamal-Hanjani, Mariana Grobler, Mariana Silva Dos Santos, Mark Johnson, Mary Wu, Matthew Singer, Matthew J. Williams, Maximiliano G. Gutierrez, Melanie Turner, Melvyn Yap, Michael Howell, Michael Hubank, Michael J. Blackman, Michael D. Buck, Michele S. Y. Tan, Michelle Lappin, Mimmi Martensson, Ming Jiang, Ming-Han C. Tsai, Ming-Shih Hwang, Mint RHTun, Miriam Molina-Arcas, Moira J. Spyer, Monica Diaz-Romero, Moritz Treeck, Namita Patel, Natalie Chandler, Neil Osborne, Nick Carter, Nicola O’Reilly, Nigel Peat, Nikhil Faulkner, Nikita Komarov, Nisha Bhardwaj, Nnennaya Kanu, Oana Paun, Ok-Ryul Song, Olga O’Neill, Pablo Romero Clavijo, Patrick Davis, Patrick Toolan-Kerr, Paul Nurse, Paul Kotzampaliris, Paul C. Driscoll, Paul R. Grant, Paula Ordonez Suarez, Peter Cherepanov, Peter Ratcliffe, Philip Hobson, Philip A. Walker, Pierre Santucci, Qu Chen, Rachael Instrell, Rachel Ambler, Rachel Ulferts, Rachel Zillwood, Raffaella Carzaniga, Rajnika Hirani, Rajvee Shah Punatar, Richard Byrne, Robert Goldstone, Robyn Labrum, Ross Hall, Rowenna Roberts, Roy Poh, Rupert Beale, Rupert Faraway, Sally Cottrell, Sam Barrell, Sam Loughlin, Samuel McCall, Samutheswari Balakrishnan, Sandra Segura-Bayona, Savita Nutan, Selvaraju Veeriah, Shahnaz Bibi, Sharon P. Vanloo, Simon Butterworth, Simon Caidan, Solene Debaisieux, Sonia Gandhi, Sophia Ward, Sophie Ridewood, Souradeep Basu, Stacey-Ann Lee, Steinar Halldorsson, Stephanie Nofal, The SAFER Investigators and Field Study Team, and The Crick COVID-19 Consortium. Estimating the effectiveness of routine asymptomatic PCR testing at different frequencies for the detection of SARS-CoV-2 infections. *BMC Medicine*, 19(1):106, April 2021. ISSN 1741-7015. doi:10.1186/s12916-021-01982-x.

- [29] Catherine F Houlihan, Nina Vora, Thomas Byrne, Dan Lewer, Gavin Kelly, Judith Heaney, Sonia Gandhi, Moira J Spyer, Rupert Beale, Peter Cherepanov, David Moore, Richard Gilson, Steve Gamblin, George Kassiotis, Laura E McCoy, Charles Swanton, Andrew Hayward, Eleni Nastouli, Jim Aitken, Zoe Allen, Rachel Ambler, Karen Ambrose, Emma Ashton, Alida Avola, Samutheswari Balakrishnan, Caitlin Barns-Jenkins, Genevieve Barr, Sam Barrell, Souradeep Basu, Rupert Beale, Clare Beesley, Nisha Bhardwaj, Shahnaz Bibi, Ganka Bineva-Todd, Dhruva Biswas, Michael J Blackman, Dominique Bonnet, Faye Bowker, Malgorzata Broncel, Claire Brooks, Michael D Buck, Andrew Buckton, Timothy Budd, Alana Burrell, Louise Busby, Claudio Bussi, Simon Butterworth, Fiona Byrne, Richard Byrne, Simon Caidan, Joanna Campbell, Johnathan Canton, Ana Cardoso, Nick Carter, Luiz Carvalho, Raffaella Carzaniga, Natalie Chandler, Qu Chen, Peter Cherepanov, Laura Churchward, Graham Clark, Bobbi Clayton, Clementina Cobolli Gigli, Zena Collins, Sally Cottrell, Margaret Crawford, Laura Cubitt, Tom Cullup, Heledd Davies, Patrick Davis, Dara Davison, Annalisa D’Avola, Vicky Dearing, Solene Debaisieux, Monica Diaz-Romero, Alison Dibbs, Jessica Diring, Paul C Driscoll, Christopher Earl, Amelia Edwards, Chris Ekin, Dimitrios Evangelopoulos, Rupert Faraway, Antony Fearn, Aaron Ferron, Eftymios Fidanis, Dan Fitz, James Fleming, Bruno Frederico, Alessandra Gaiba, Anthony Gait, Steve Gamblin, Sonia Gandhi, Liam Gaul, Helen M Golding, Jacki Goldman, Robert Goldstone, Belen Gomez Dominguez, Hui Gong, Paul R Grant, Maria Greco, Mariana Grobler, Anabel Guedan, Maximiliano G Gutierrez, Fiona Hackett, Ross Hall, Steinar Halldorsson, Suzanne Harris, Sugera Hashim, Lyn Healy, Judith Heaney, Susanne Herbst,

Graeme Hewitt, Theresa Higgins, Steve Hindmarsh, Rajnika Hirani, Joshua Hope, Elizabeth Horton, Beth Hoskins, Catherine F Houlihan, Michael Howell, Louise Howitt, Jacqueline Hoyle, Mint R Htun, Michael Hubank, Hector Huerga Encabo, Deborah Hughes, Jane Hughes, Almaz Huseynova, Ming-Shih Hwang, Rachael Instrell, Deborah Jackson, Mariam Jamal-Hanjani, Lucy Jenkins, Ming Jiang, Mark Johnson, Leigh Jones, Nnennaya Kanu, George Kassiotis, Louise Kiely, Anastacio King Spert Teixeira, Stuart Kirk, Svend Kjaer, Ellen Knuepfer, Nikita Komarov, Paul Kotzampaltiris, Konstantinos Kousis, Tammy Krylova, Ania Kucharska, Robyn Labrum, Catherine Lambe, Michelle Lappin, Stacey-Ann Lee, Andrew Levett, Lisa Levett, Marcel Levi, Hon-Wing Liu, Sam Loughlin, Wei-Ting Lu, James I MacRae, Akshay Madoo, Julie A Marczak, Mimmi Martensson, Thomas Martinez, Bishara Marzook, John Matthews, Joachim M Matz, Samuel McCall, Laura E McCoy, Fiona McKay, Edel C McNamara, Carlos M Minutti, Gita Mistry, Miriam Molina-Arcas, Beatriz Montaner, Kylie Montgomery, Catherine Moore, David Moore, Anastasia Moraiti, Lucia Moreira-Teixeira, Joyita Mukherjee, Cristina Naceur-Lombardelli, Eleni Nastouli, Aileen Nelson, Jerome Nicod, Luke Nightingale, Stephanie Nofal, Paul Nurse, Savita Nutan, Caroline Oedekoven, Anne O'Garra, Jean D O'Leary, Jessica Olsen, Olga O'Neill, Paula Ordonez Suarez, Nicola O'Reilly, Neil Osborne, Amar Pabari, Aleksandra Pajak, Venizelos Papayannopoulos, Namita Patel, Yogen Patel, Oana Paun, Nigel Peat, Laura Peces-Barba Castano, Ana Perez Caballero, Jimena Perez-Lloret, Magali S Perrault, Abigail Perrin, Roy Poh, Enzo Z Poirier, James M Polke, Marc Pollitt, Lucia Prieto-Godino, Alize Proust, Rajvee Shah Punatar, Clinda Puvirajasinghe, Christophe Queval, Vijaya Ramachandran, Abhinay Ramaprasad, Peter Ratcliffe, Laura Reed, Caetano Reis e Sousa, Kayleigh Richardson, Sophie Ridewood, Rowenna Roberts, Angela Rodgers, Pablo Romero Clavijo, Annachiara Rosa, Alice Rossi, Chloe Roustan, Andrew Rowan, Erik Sahai, Aaron Sait, Katarzyna Sala, Theo Sanderson, Pierre Santucci, Fatima Sardar, Adam Sateriale, Jill A Saunders, Chelsea Sawyer, Anja Schlott, Edina Schweighoffer, Sandra Segura-Bayona, Joe Shaw, Gee Yen Shin, Mariana Silva Dos Santos, Margaux Silvestre, Matthew Singer, Daniel M Snell, Ok-Ryul Song, Moira J Spyer, Louisa Steel, Amy Strange, Adrienne E Sullivan, Charles Swanton, Michele SY Tan, Zoe H Tautz-Davis, Effie Taylor, Gunes Taylor, Harriet B Taylor, Alison Taylor-Beadling, Fernanda Teixeira Subtil, Berta Terré Torras, Patrick Toolan-Kerr, Francesca Torelli, Tea Toteva, Moritz Treeck, Hadija Trojer, Ming-Han C Tsai, James MA Turner, Melanie Turner, Jernej Ule, Rachel Ulferts, Sharon P Vanloo, Selvaraju Veeriah, Subramanian Venkatesan, Karen Vousden, Andreas Wack, Claire Walder, Philip A Walker, Yiran Wang, Sophia Ward, Catharina Wenman, Luke Williams, Matthew J Williams, Wai Keong Wong, Joshua Wright, Mary Wu, Lauren Wynne, Zheng Xi-ang, Melvyn Yap, Julian A Zagalak, Davide Zecchin, Rachel Zillwood, Rebecca Matthews, Abigail Severn, Sajida Adam, Louise Enfield, Angela McBride, Kathleen Gärtner, Sarah Edwards, Fabiana Lorencatto, Susan Michie, Ed Manley, Maryam Shahmanesh, Hinal Lukha, Paulina Prymas, Hazel McBain, Robert Shortman, Leigh Wood, Claudia Davies, Bethany Williams, Kevin W Ng, Georgina H Cornish, Nikhil Faulkner, Andrew Riddell, Philip Hobson, Ana Agua-Doce, Kerol Bartolovic, Emma Russell, Lotte Carr, Emilie Sanchez, Daniel Frampton, Matthew Byott, Stavroula M Paraskevopoulou, Elise Crayton, Carly Meyer, Nina Vora, Triantafylia Gkouleli, Andrea Stoltenberg, Veronica Ranieri, Tom Byrne, Dan Lewer, Andrew Hayward, Richard Gilson, Gavin Kelly, Fiona Roberts, and Emine Hatipoglu. Pandemic peak SARS-CoV-2 infection and seroconversion rates in London frontline health-care workers. *The Lancet*, 396(10246):e6–e7, July 2020. ISSN 01406736. doi:[10.1016/S0140-6736\(20\)31484-7](https://doi.org/10.1016/S0140-6736(20)31484-7).

- [30] M. Hucka, A. Finney, H. M. Sauro, H. Bolouri, J. C. Doyle, H. Kitano, A. P. Arkin, B. J. Bornstein, D. Bray, A. Cornish-Bowden, A. A. Cuellar, S. Dronov, E. D. Gilles, M. Ginkel, V. Gor, I. I. Goryanin, W. J. Hedley, T. C. Hodgman, J.-H. Hofmeyr, P. J. Hunter, N. S. Juty, J. L. Kasberger, A. Kremling, U. Kummer, N. Le Novère, L. M. Loew, D. Lucio, P. Mendes, E. Minch, E. D. Mjolsness, Y. Nakayama, M. R. Nelson, P. F. Nielsen, T. Sakurada, J. C. Schaff, B. E. Shapiro, T. S. Shimizu, H. D. Spence, J. Stelling, K. Takahashi, M. Tomita, J. Wagner, J. Wang, and the rest of the SBML Forum. The systems biology markup language (SBML): a medium for

- representation and exchange of biochemical network models. *Bioinformatics*, 19(4):524–531, March 2003. ISSN 1367-4803. doi:[10.1093/bioinformatics/btg015](https://doi.org/10.1093/bioinformatics/btg015).
- [31] C Anthony Hunt, Glen E P Ropella, Tai Ning Lam, Jonathan Tang, Sean H J Kim, Jesse A Engelberg, and Shahab Sheikh-Bahaei. At the biological modeling and simulation frontier. *Pharmaceutical research*, 26(11):2369–2400, November 2009. ISSN 0724-8741. doi:[10.1007/s11095-009-9958-3](https://doi.org/10.1007/s11095-009-9958-3). URL <https://europepmc.org/articles/PMC2763179>.
- [32] Sarah M Keating, Dagmar Waltemath, Matthias König, Fengkai Zhang, Andreas Dräger, Claudine Chaouiya, Frank T Bergmann, Andrew Finney, Colin S Gillespie, Tomáš Helikar, Stefan Hoops, Rahuman S Malik-Sheriff, Stuart L Moodie, Ion I Moraru, Chris J Myers, Aurélien Naldi, Brett G Olivier, Sven Sahle, James C Schaff, Lucian P Smith, Maciej J Swat, Denis Thieffry, Leandro Watanabe, Darren J Wilkinson, Michael L Blinov, Kimberly Begley, James R Faeder, Harold F Gómez, Thomas M Hamm, Yuichiro Inagaki, Wolfram Liebermeister, Allyson L Lister, Daniel Lucio, Eric Mjolsness, Carole J Proctor, Karthik Raman, Nicolas Rodriguez, Clifford A Shaffer, Bruce E Shapiro, Joerg Stelling, Neil Swainston, Naoki Tanimura, John Wagner, Martin Meier-Schellersheim, Herbert M Sauro, Bernhard Palsson, Hamid Bolouri, Hiroaki Kitano, Akira Funahashi, Henning Hermjakob, John C Doyle, Michael Hucka, Richard R Adams, Nicholas A Allen, Bastian R Angermann, Marco Antonioti, Gary D Bader, Jan Červený, Mélanie Courtot, Chris D Cox, Piero Dalle Pezze, Emek Demir, William S Denney, Harish Dharuri, Julien Dorier, Dirk Drasdo, Ali Ebrahim, Johannes Eichner, Johan Elf, Lukas Endler, Chris T Evelo, Christoph Flamm, Ronan MT Fleming, Martina Fröhlich, Mihai Glont, Emanuel Gonçalves, Martin Golebiewski, Hovakim Grabski, Alex Gutteridge, Damon Hachmeister, Leonard A Harris, Benjamin D Heavner, Ron Henkel, William S Hlavacek, Bin Hu, Daniel R Hyduke, Hidde Jong, Nick Juty, Peter D Karp, Jonathan R Karr, Douglas B Kell, Roland Keller, Ilya Kiselev, Steffen Klamt, Edda Klipp, Christian Knüpfer, Fedor Kolpakov, Falko Krause, Martina Kutmon, Camille Laibe, Conor Lawless, Lu Li, Leslie M Loew, Rainer Machne, Yukiko Matsuoka, Pedro Mendes, Huaiyu Mi, Florian Mittag, Pedro T Monteiro, Kedar Nath Natarajan, Poul MF Nielsen, Tramy Nguyen, Alida Palmisano, Jean-Baptiste Pettit, Thomas Pfau, Robert D Phair, Tomas Radivoyevitch, Johann M Rohwer, Oliver A Ruebenacker, Julio Saez-Rodriguez, Martin Scharm, Henning Schmidt, Falk Schreiber, Michael Schubert, Roman Schulte, Stuart C Sealfon, Kieran Smallbone, Sylvain Soliman, Melanie I Stefan, Devin P Sullivan, Koichi Takahashi, Bas Teusink, David Tolnay, Ibrahim Vazirabad, Axel Kamp, Ulrike Wittig, Clemens Wrzodek, Finja Wrzodek, Ioannis Xenarios, Anna Zhukova, and Jeremy Zucker. SBML Level 3: an extensible format for the exchange and reuse of biological models. *Molecular Systems Biology*, 16(8):e9110, August 2020. ISSN 1744-4292. doi:[10.15252/msb.20199110](https://doi.org/10.15252/msb.20199110). Publisher: John Wiley & Sons, Ltd.
- [33] Cliff C. Kerr, Robyn M. Stuart, Dina Mistry, Romesh G. Abeysuriya, Katherine Rosenfeld, Gregory R. Hart, Rafael C. Núñez, Jamie A. Cohen, Prashanth Selvaraj, Brittany Hagedorn, Lauren George, Michal Jastrzebski, Amanda S. Izzo, Greer Fowler, Anna Palmer, Dominic Delpont, Nick Scott, Sherrie L. Kelly, Caroline S. Bennette, Bradley G. Wagner, Stewart T. Chang, Assaf P. Oron, Edward A. Wenger, Jasmina Panovska-Griffiths, Michael Famulare, and Daniel J. Klein. Covasim: An agent-based model of COVID-19 dynamics and interventions. *PLOS Computational Biology*, 17(7):e1009149, July 2021. ISSN 1553-7358. doi:[10.1371/journal.pcbi.1009149](https://doi.org/10.1371/journal.pcbi.1009149). Publisher: Public Library of Science.
- [34] D.M. Kreps, M. Kreps, and P.E.H.P.E.G.S.B.D.M. Kreps. *A Course in Microeconomic Theory*. Princeton University Press, 1990. ISBN 9780691042640. URL <https://books.google.com/books?id=yLmkDwAAQBAJ>.
- [35] Jean Krivine, Robin Milner, and Angelo Troina. Stochastic Bigraphs. *Electronic Notes in Theoretical Computer Science*, 218:73–96, October 2008. ISSN 1571-0661. doi:[10.1016/j.entcs.2008.10.006](https://doi.org/10.1016/j.entcs.2008.10.006).

- [36] Nike J. Kräutler, Dan Suan, Danyal Butt, Katherine Bourne, Jana R. Hermes, Tyani D. Chan, Christopher Sundling, Warren Kaplan, Peter Schofield, Jennifer Jackson, Antony Basten, Daniel Christ, and Robert Brink. Differentiation of germinal center B cells into plasma cells is initiated by high-affinity antigen and completed by Tfh cells. *Journal of Experimental Medicine*, 214(5): 1259–1267, May 2017. ISSN 0022-1007, 1540-9538. doi:[10.1084/jem.20161533](https://doi.org/10.1084/jem.20161533).
- [37] Nicolas Le Novère, Benjamin Bornstein, Alexander Broicher, Mélanie Courtot, Marco Donizelli, Harish Dharuri, Lu Li, Herbert Sauro, Maria Schilstra, Bruce Shapiro, Jacky L. Snoep, and Michael Hucka. BioModels Database: a free, centralized database of curated, published, quantitative kinetic models of biochemical and cellular systems. *Nucleic Acids Research*, 34(suppl_1):D689–D691, January 2006. ISSN 0305-1048. doi:[10.1093/nar/gkj092](https://doi.org/10.1093/nar/gkj092).
- [38] Catherine M. Lloyd, James R. Lawson, Peter J. Hunter, and Poul F. Nielsen. The CellML Model Repository. *Bioinformatics*, 24(18):2122–2123, September 2008. ISSN 1367-4803. doi:[10.1093/bioinformatics/btn390](https://doi.org/10.1093/bioinformatics/btn390). URL <https://doi.org/10.1093/bioinformatics/btn390>.
- [39] Filip Logist, Boris Houska, Moritz Diehl, and Jan F Van Impe. Robust multi-objective optimal control of uncertain (bio) chemical processes. *Chemical engineering science*, 66(20):4670–4682, 2011.
- [40] David Manheim, Margaret Chamberlin, Osonde Osoba, Raffaele Vardavas, and Melinda Moore. *Improving Decision Support for Infectious Disease Prevention and Control: Aligning Models and Other Tools with Policymakers’ Needs*. RAND Corporation, 2016. ISBN 978-0-8330-9550-3 978-0-8330-9630-2. doi:[10.7249/RR1576](https://doi.org/10.7249/RR1576).
- [41] Hongyu Miao, Joseph A. Hollenbaugh, Martin S. Zand, Jeanne Holden-Wiltse, Tim R. Mosmann, Alan S. Perelson, Hulin Wu, and David J. Topham. Quantifying the Early Immune Response and Adaptive Immune Response Kinetics in Mice Infected with Influenza A Virus. *Journal of Virology*, 84(13):6687–6698, July 2010. ISSN 0022-538X, 1098-5514. doi:[10.1128/JVI.00266-10](https://doi.org/10.1128/JVI.00266-10).
- [42] Sebastian Mirschel, Katrin Steinmetz, Michael Rempel, Martin Ginkel, and Ernst Dieter Gilles. ProMoT: modular modeling for systems biology. *Bioinformatics*, 25(5):687–689, 01 2009. ISSN 1367-4803. doi:[10.1093/bioinformatics/btp029](https://doi.org/10.1093/bioinformatics/btp029). URL <https://doi.org/10.1093/bioinformatics/btp029>.
- [43] Philippe Nimmegheers, Dries Telen, Mickey Beetens, Filip Logist, and Jan Van Impe. Parametric uncertainty propagation for robust dynamic optimization of biological networks. In *2016 American Control Conference (ACC)*, pages 6929–6934, 2016. doi:[10.1109/ACC.2016.7526764](https://doi.org/10.1109/ACC.2016.7526764).
- [44] Timothy C. Reluga. Game theory of social distancing in response to an epidemic. *PLOS Computational Biology*, 6(5):1–9, 05 2010. doi:[10.1371/journal.pcbi.1000793](https://doi.org/10.1371/journal.pcbi.1000793). URL <https://doi.org/10.1371/journal.pcbi.1000793>.
- [45] Roberto A. Saenz, Michelle Quinlivan, Debra Elton, Shona MacRae, Anthony S. Blunden, Jennifer A. Mumford, Janet M. Daly, Paul Digard, Ann Cullinane, Bryan T. Grenfell, John W. McCauley, James L. N. Wood, and Julia R. Gog. Dynamics of Influenza Virus Infection and Pathology. *Journal of Virology*, 84(8):3974–3983, April 2010. ISSN 0022-538X, 1098-5514. doi:[10.1128/JVI.02078-09](https://doi.org/10.1128/JVI.02078-09).
- [46] Robert E. Schapire. The strength of weak learnability, 1990.
- [47] Robert E. Schapire and Yoav Freund. *Game Theory, Online Learning, and Boosting*, pages 141–174. MIT Press, 2012.

- [48] Alessandro Sette and Shane Crotty. Adaptive immunity to SARS-CoV-2 and COVID-19. *Cell*, 184(4):861–880, February 2021. ISSN 0092-8674, 1097-4172. doi:10.1016/j.cell.2021.01.007. Publisher: Elsevier.
- [49] Christina D. Smolke. Building outside of the box: iGEM and the BioBricks Foundation. *Nature Biotechnology*, 27(12):1099–1102, December 2009. ISSN 1546-1696. doi:10.1038/nbt1209-1099.
- [50] Carole H. Sudre, Benjamin Murray, Thomas Varsavsky, Mark S. Graham, Rose S. Penfold, Ruth C. Bowyer, Joan Capdevila Pujol, Kerstin Klaser, Michela Antonelli, Liane S. Canas, Erika Molteni, Marc Modat, M. Jorge Cardoso, Anna May, Sajaysurya Ganesh, Richard Davies, Long H. Nguyen, David A. Drew, Christina M. Astley, Amit D. Joshi, Jordi Merino, Neli Tsereteli, Tove Fall, Maria F. Gomez, Emma L. Duncan, Cristina Menni, Frances M. K. Williams, Paul W. Franks, Andrew T. Chan, Jonathan Wolf, Sebastien Ourselin, Tim Spector, and Claire J. Steves. Attributes and predictors of long COVID. *Nature Medicine*, 27(4):626–631, April 2021. ISSN 1078-8956, 1546-170X. doi:10.1038/s41591-021-01292-y.
- [51] Kelvin Kai-Wang To, Owen Tak-Yin Tsang, Wai-Shing Leung, Anthony Raymond Tam, Tak-Chiu Wu, David Christopher Lung, Cyril Chik-Yan Yip, Jian-Piao Cai, Jacky Man-Chun Chan, Thomas Shiu-Hong Chik, Daphne Pui-Ling Lau, Chris Yau-Chung Choi, Lin-Lei Chen, Wan-Mui Chan, Kwok-Hung Chan, Jonathan Daniel Ip, Anthony Chin-Ki Ng, Rosana Wing-Shan Poon, Cui-Ting Luo, Vincent Chi-Chung Cheng, Jasper Fuk-Woo Chan, Ivan Fan-Ngai Hung, Zhiwei Chen, Honglin Chen, and Kwok-Yung Yuen. Temporal profiles of viral load in posterior oropharyngeal saliva samples and serum antibody responses during infection by SARS-CoV-2: an observational cohort study. *The Lancet Infectious Diseases*, 20(5):565–574, May 2020. ISSN 1473-3099, 1474-4457. doi:10.1016/S1473-3099(20)30196-1.
- [52] Ludwig Von Bertalanffy. The Theory of Open Systems in Physics and Biology. *Science*, 111(2872):23–29, 1950. ISSN 0036-8075. URL <https://www.jstor.org/stable/1676073>. Publisher: American Association for the Advancement of Science.
- [53] W. Waites, M. Cavaliere, D. Manheim, J. Panovska-Griffiths, and V. Danos. Rule-based epidemic models. *Journal of Theoretical Biology*, page 110851, July 2021. ISSN 0022-5193. doi:10.1016/j.jtbi.2021.110851.
- [54] William Waites, Carl AB Pearson, Katherine M. Gaskell, Thomas House, Lorenzo Pellis, Marina Johnson, Victoria Gould, Adam Hunt, Neil RH Stone, Ben Kasstan, Tracey Chantler, Sham Lal, Chrissy h Roberts, David Goldblatt, CMMID COVID-19 Working Group, Michael Marks, and Rosalind M. Eggo. Transmission dynamics of SARS-CoV-2 in a strictly-Orthodox Jewish community in the UK. Technical report, medRxiv, October 2021.
- [55] Abraham Wald. Statistical decision functions. *Nature*, 167:1044–1044, 1951.
- [56] Kieran A. Walsh, Karen Jordan, Barbara Clyne, Daniela Rohde, Linda Drummond, Paula Byrne, Susan Ahern, Paul G. Carty, Kirsty K. O’Brien, Eamon O’Murchu, Michelle O’Neill, Susan M. Smith, Máirín Ryan, and Patricia Harrington. SARS-CoV-2 detection, viral load and infectivity over the course of an infection. *Journal of Infection*, 81(3):357–371, September 2020. ISSN 0163-4453. doi:10.1016/j.jinf.2020.06.067.
- [57] Veronika I Zarnitsyna, Juliano Ferrari Gianlupi, Amit Hagar, Tj Sego, and James A Glazier. Advancing therapies for viral infections using mechanistic computational models of the dynamic interplay between the virus and host immune response. *Current Opinion in Virology*, 50:103–109, October 2021. ISSN 18796257. doi:10.1016/j.coviro.2021.07.007.

A The combined model

This model contains all of the rules that are described above, in machine-readable form.

```

1 // -*- mode: kappa -*-
2
3 // Rule-based model of a multi-scale epidemic consisting of an adaptive
4 // immune response and transmission
5 //
6 // Copyright 2021 William Waites <william.waites@lshtm.ac.uk>
7 //
8 // This program is free software: you can redistribute it and/or modify
9 // it under the terms of the GNU General Public License as published by
10 // the Free Software Foundation, either version 3 of the License, or
11 // (at your option) any later version.
12 //
13 // This program is distributed in the hope that it will be useful,
14 // but WITHOUT ANY WARRANTY; without even the implied warranty of
15 // MERCHANTABILITY or FITNESS FOR A PARTICULAR PURPOSE. See the
16 // GNU General Public License for more details.
17 //
18 // You should have received a copy of the GNU General Public License
19 // along with this program. If not, see <https://www.gnu.org/licenses/>.
20
21 // This program is written in the Stratified Kappa language which is
22 // essentially a version of Kappa as understood by the KaSim simulator
23 // with a pre-processor that allows generation of rules from fragments
24 // of python code.
25
26 // exec
27 ## res is passed in as a parameter and controls the resolution
28 ## of counters in the simulation, and headroom to obviate truncation.
29 ## typical values are 10 and 10.
30 ## need to coerce to an integer because they may have been passed
31 ## in as a floating point number.
32 res = int(res)
33 head = int(headroom)
34 // end exec
35
36 %agent: Virus(person count{=0 / += $res+head$})
37 %agent: Person(bcell, virus)
38 %agent: BCell(person antibody affinity{=0 / += $res$})
39 %agent: Antibody(bcell count{=0 / += $res+head$})
40
41 // Eq. 3.1 -- virus proliferation
42 // iterate for i in range(1,res+head):
43 'virus_$$i$' Virus(person[_], count{=$i$ / += 1}) @ k_virus/$res$
44 // end iterate
45
46 // Eq. 3.2 -- allocation of B-cell population
47 't_cell' Person(bcell[.], virus[_]), . \
48     -> Person(bcell[1], virus[_]), BCell(person[1]) \
49     @ inf
50
51 // Eq. 3.3 -- allocation of antibody population
52 'activate' Person(bcell[1], virus[_]), \
53     BCell(person[1], antibody[.]), \
54     .
55     -> Person(bcell[1], virus[_]), \

```

```

56         BCell(person[1], antibody[2]), \
57         Antibody(bcell[2], count{=0}) \
58     @ inf
59
60 // Eq. 3.4 -- affinity maturation
61 // iterate for i in range(res):
62 'mature_$$' Person(bcell[1], virus[2]), \
63         BCell(person[1], affinity{=$$ / += 1}), \
64         Virus(person[2], count{=v}) \
65     @ v*k_mature/$res$
66 // end iterate
67
68 // Eq. 3.5 -- antibody production
69 // iterate for i in range(res+head):
70 'anti_$$' Person(bcell[1], virus[_]), \
71         BCell(person[1], antibody[2], affinity{=a}), \
72         Antibody(bcell[2], count{=$$ / += 1}) \
73     @ a*k_resp/$res$
74 // end iterate
75
76 // Eq. 3.6 -- virus neutralisation
77 // iterate for i in range(1,res+head+1):
78 'neutralise_$$' Person(bcell[1], virus[2]), \
79         BCell(person[1], antibody[3]), \
80         Antibody(bcell[3], count{=c}), \
81         Virus(person[2], count{=$$ / -= 1}) \
82     @ c*k_bind/$res$
83 // end iterate
84
85 // Eq. 3.7 -- clearing of the virus
86 'clear' Person(virus[1]), Virus(person[1], count{=0}) -> Person(virus[.]), . @
87     k_clear
88
89 // Eq. 3.8 -- waning
90 'waning' Person(bcell[1], virus[.]), \
91         BCell(person[1], antibody[2]), \
92         Antibody(bcell[2], count{>=1 / -= 1}) @ k_wane
93
94 // Eq. 4.1 -- transmission
95 'infection' Person(virus[1]), Virus(person[1], count{=c}), \
96         Person(virus[.]), . \
97     -> Person(virus[1]), Virus(person[1]), \
98         Person(virus[2]), Virus(person[2], count{=1}) \
99     @ c*contacts*beta/N
100 // Initial conditions of a simulation -- rapidly allocate free virus populations
101 // to people
102 'start' Person(virus[.]), Virus(person[.]) -> Person(virus[1]), Virus(person[1]) @
103     inf
104
105 // Eq. 3.9 -- standard epidemiological observables
106 %obs: S |Person(bcell[.], virus[.])|
107 %obs: I |Person(virus[.])|
108 %obs: R |Person(bcell[_], virus[.])|
109
110 // Observables for various counters
111 // iterate for i in range(res+head+1):
112 %obs: V$$ |Virus(person[_], count{=$$})|
113 // end iterate

```



```
112 // iterate for i in range(res+head+1):
113 %obs: A$i$ |Antibody(count{=$i$})|
114 // end iterate
115 // iterate for i in range(res+1):
116 %obs: B$i$ |BCell(affinity{=$i$})|
117 // end iterate
118
119 // inital conditions
120 %init: N   Person()
121 %init: IO  Virus(count{=1})
```